Crystal Engineering as a Tool for Directed Radiationless Energy Transfer in Layered {Λ-[Ru(bpy)$_3$]Δ-[Os(bpy)$_3$]}(PF$_6$)$_4$

Josef Breu,*,† Cornelius Kratzer,‡ and Hartmut Yersin*,‡

Contribution from the Institut für Anorganische Chemie and the Institut für Physikalische Chemie, Universität Regensburg, D-93040 Regensburg, Germany

Received August 26, 1999

Abstract: New types of crystal structures with new physical properties such as energy harvesting can be engineered by exploiting the potentiality of chiral recognition. In the proposed strategy one takes advantage of the possibility that in true racemates one enantiomeric component in the crystal packing may be replaced by a different molecule of the same chirality and similar shape. This opens the path to a number of new properties. In the present investigation, we demonstrate that a system can be engineered, in which homochiral layers of Λ-[Ru(bpy)$_3$]$^{2+}$ rigorously alternate with homochiral layers of Δ-[Os(bpy)$_3$]$^{2+}$. This arrangement is realized in {Λ-[Ru(bpy)$_3$]Δ-[Os(bpy)$_3$]}(PF$_6$)$_4$. Due to the deliberately introduced lower dimensionality, the new crystalline system exhibits fascinating properties, in particular with respect to an interplay of processes of interlayer and intralayer radiationless energy transfer. Interestingly, in this system it is possible to achieve a controlled accumulation of excitation energy on a single crystallographic Δ-[Os(bpy)$_3$]$^{2+}$ site. Moreover, the excitation energy is absorbed in a wide range from the UV to the red side of the visible by both Λ-[Ru(bpy)$_3$]$^{2+}$ and Δ-[Os(bpy)$_3$]$^{2+}$ units, and one observes an intense red/infrared and highly resolved emission only of the low-energy Δ-[Os(bpy)$_3$]$^{2+}$ site, irrespective of the excitation wavelength used. The crystal structure of this newly engineered compound is determined for both the room-temperature phase ($P32$, $a = 10.7012(5)$ Å, $c = 16.3490(10)$ Å) as well as for the low-temperature phase ($P3$, $a = 18.4189(10)$ Å, $c = 16.2309(9)$ Å).

1. Introduction

Physical properties of a solid, such as conductivity, color, luminescence characteristics, etc., depend critically on its crystal structure. Thus, if one is able to control the structure of a solid, one can also influence its physical properties. Crystal engineering, the design of molecular solids with specified packing architectures,[1] is therefore a rapidly developing field.[2−5] Most crystal engineering strategies start with the layout of the molecular entity[6] by employing functional groups to achieve the controlled molecule-to-crystal transcription. This approach seeks to establish a connection between the molecular and the supramolecular structure (crystal). Contrary to this, we present a strategy that sets out at a known crystal structure with a given topology. This supramolecular structure is deliberately designed and significantly altered by a controlled reduction of the space group symmetry of the packing arrangement. Such parent group−subgroup relations between space groups have previously only been used as a tool to order topologically equivalent stuctures.[7,8] The crystal engineering approach starting from the supramolecular side is conceptually different and it is of general interest because it does not rely on relatively strong and directional intermolecular interactions such as classical hydrogen bonds. Here, dispersion and weak $\pi-\pi$ interactions are fully sufficient to tune the topology and to establish the crystal structure. In the present investigation, we use the group−subgroup strategy to manipulate packing motifs of the luminescent [Ru(bpy)$_3$]$^{2+}$ and [Os(bpy)$_3$]$^{2+}$ complexes (bpy = 2,2′-bipyridine) for a controlled and directed radiationless energy transfer.

These and related compounds exhibit an enormous potential for new applications due to their photophysical and photochemical properties (compare ref 9 and references therein). In particular, it is currently of high interest to design molecules or supramolecular arrangements consisting of [Ru(bpy)$_3$]$^{2+}$ and [Os(bpy)$_3$]$^{2+}$ or related units by which excitation energy can deliberately be directed from antenna units (donors) to acceptors through radiationless energy transfer. Such processes, applying Ru(II) and Os(II) compounds, have been investigated for more than a decade.[10−18] Interestingly, the newly engineered {Λ-[Ru-

† Institut für Anorganische Chemie.
‡ Institut für Physikalische Chemie.

(1) Desiraju, G. R. Crystal Engineering. In *Materials Science Monographs*; Elsevier: Amsterdam, 1989;Vol. 54.
(2) Desiraju, G. R. *Curr. Opin. Solid State Mater. Sci.* **1997**, *2*, 451.
(3) Desiraju, G. R.; Krishnamohan Sharma, C. V. In *The Crystal as a Supramolecular Entity*; Desiraju, G. R., Ed.; John Wiley & Sons: Chichester, 1996; p 31.
(4) Braga, D.; Grepioni, F.; Desiraju, G. R. *Chem. Rev.* **1998**, *98*, 1375.
(5) Aakeröy, C. B. *Acta Crystallogr. B* **1997**, *53*, 569.
(6) Desiraju, G. R. *Angew. Chem., Int. Ed. Engl.* **1995**, *34*, 2311.
(7) Bärnighausen, H. *Match* **1980**, *9*, 139.
(8) Müller, U. *Acta Crystallogr. B* **1980**, *36*, 1075.
(9) Yersin, H.; Humbs, W.; Strasser, J. In *Electronic and Vibronic Spectra of Transition Metal Complexes*; Yersin, H., Ed.; Topics in Current Chemistry 191; Springer: Berlin, 1997; Vol. II, p 153.
(10) Yersin, H.; Braun, D.; Gallhuber, E.; Hensler, G. *Ber. Bunsen-Ges. Phys. Chem.* **1987**, *91*, 1228.
(11) Yersin, H.; Hensler, G.; Gallhuber, E. *J. Luminesc.* **1988**, *40−41*, 676.
(12) De Cola, L.; Barigelletti, F.; Balzani, V.; Hage, R.; Haasnoot, J. G.; Reedijk, J.; Vos, J. G. *Chem. Phys. Lett.* **1991**, *178*, 491.
(13) Furue, M.; Maruyama, K.; Kanematsu, Y.; Kushida, T.; Kamachi, M. *Coord. Chem. Rev.* **1994**, *132*, 201.
(14) Belser, P.; Bernhard, S.; Jandrasics, E.; von Zelewsky, A.; De Cola, L.; Balzani, V. *Coord. Chem. Rev.* **1997**, *159*, 1.
(15) Devenny, M.; Worl, L. A.; Gould, S.; Guadalupe, A.; Sullivan, B. P.; Caspar, J. V.; Leasure, R. L.; Gardner, J. R.; Meyer, T. J. *J. Phys. Chem. A* **1997**, *101*, 4535.
(16) Grosshenny, V.; Harriman, A.; Ziessel, R. *Angew. Chem.* **1995**, *107*, 1211.

10.1021/ja993104m CCC: $19.00 © 2000 American Chemical Society
Published on Web 03/02/2000

(bpy)$_3$]Δ-[Os(bpy)$_3$]}(PF$_6$)$_4$ structure shows specific effects which allow us to accumulate energy at a distinct crystallographic site and to obtain highly informative, site-selective emission spectra, irrespectively of the applied excitation wavelength. These properties are reported here for the first time.

The paper is organized as follows: After the experimental section 2, structural aspects are discussed in section 3. Section 4 presents the effects of a directed radiationless energy transfer. Finally, section 5 gives a short conclusion.

2. Experimental Section

Synthesis. [M(bpy)$_3$]Cl$_2$ (M = Ru, Os) salts were synthesized according to published methods.[19,20] Resolution of the antipodes was achieved by a modification of the procedure of Brandt, Dwyer, and Gyarfas using potassium antimonyl tartrate.[21] Optical purity was further increased by repeated recrystallization of the resulting bromide salts. Optical rotations have been determined for the iodide salts. The values obtained for Λ-[Ru(bpy)$_3$]I$_2$, $[\alpha]^{20}_D$ +834°, and Δ-[Os(bpy)$_3$]I$_2$, $[\alpha]^{20}_{546.1}$ −2075°, compare well with the literature values of $[\alpha]^{20}_D$ +819° (ref 22) and $[\alpha]^{20}_{546.1}$ ca. −2200° (ref 23), respectively. However, the optical purity of the starting enantiomers even does not influence the optical purity of {Λ-[Ru(bpy)$_3$]Δ-[Os(bpy)$_3$]}(PF$_6$)$_4$, since the pseudoracemate is less soluble than the enantiomeric structures of the pure compounds. Therefore {Λ-[Ru(bpy)$_3$]Δ-[Os(bpy)$_3$]}(PF$_6$)$_4$ is enantiomerically pure, a fact that is also indicated by a Flack *x* parameter[24] of −0.01(1). *x* is the fractional contribution of the inverted component of a "racemic twin". It is expected to be zero for the stereochemically correct structure and unity for the inverted structure. The hexafluorophosphate salts were obtained by metathesis. Suitable single crystals of {Λ-[Ru(bpy)$_3$]Δ-[Os(bpy)$_3$]}(PF$_6$)$_4$ were obtained by slow evaporation from acetonitrile/ethanol (1:1) at ambient temperature.

Spectroscopy. The emission measurements were carried out with single crystals placed on a copper tongue and introduced into a helium bath cryostat, which was cooled to T = 1.3 K by pumping off the helium. For excitation, an argon ion laser (Coherent, λ_{exc} = 457.9 nm), a nitrogen laser (Lasertechnik Berlin, λ_{exc} = 337.1 nm), and a dye laser (Lambda Physik FL2000, nominal line half-width 0.15 cm^{-1}) pumped by a Nd:YAG laser (SL803 Spectron), respectively, were used. To avoid heating effects, the laser intensities were strongly attenuated by filters. The optical setup is described elsewhere.[25,26] The emission decay was registered by use of a fast multiscaler (minimum dwell time 0.5 ns/channel) combined with a multichannel data processor (FAST, D-82041 Oberhaching). For further details see ref 27.

Crystal Structure Analyses. (a) *β*-{Λ-[Ru(bpy)$_3$]Δ-[Os(bpy)$_3$]}-(PF$_6$)$_4$: Crystal data: T = 203(1) K, $C_{60}H_{48}N_{12}F_{24}P_4OsRu$, M = 1808.28, trigonal, *P*32 (No. 150), a = 10.7012(5) Å, c = 16.3490(10) Å, V = 1621.39(15) Å^3, Z = 1, D_x = 1.852 gcm^{-3}, Mo Kα radiation (λ = 0.71069 Å), graphite monochromator, μ = 2.41 mm^{-1}, dark blue, hexagonal prism (0.52 × 0.11 × 0.10 mm). Data collection: Stoe IPDS diffractometer, 25038 reflections measured, 3116 independent reflections, R_{int} = 0.058, 2682 observed reflections ($I_o > 2\sigma(I_o)$), θ_{max} = 29.9°, h = −14 → 14, k = −14 → 14, l = −22 → 22, numerical absorption correction: T_{min} = 0.4934, T_{max} = 0.8414. Refinement: refined on F^2 using all reflections (SHELXL[28]), H-atoms "riding", $wR(F^2)$ = 0.0480, $R(F)$ = 0.0313, S = 0.862, Flack-parameter[24] −0.01(1), 155 parameters, $(\Delta/\sigma)_{max} < 0.001$, $\Delta\rho_{max}$ = 0.550 e Å^{-3}, $\Delta\rho_{min}$ = −0.564 e Å^{-3}.

(b) α-{Λ-[Ru(bpy)$_3$]Δ-[Os(bpy)$_3$]}(PF$_6$)$_4$: Crystal data: T = 105(1) K, $C_{180}H_{144}N_{36}F_{72}P_{12}$ Os_3Ru_3, M = 5424.84, trigonal, *P*3 (No. 143), a = 18.4189(10) Å, c = 16.2309(9) Å, V = 4768.7(5) Å^3, Z = 1, D_x = 1.889 g cm^{-3}, Mo Kα radiation (λ = 0.71069 Å), graphite monochromator, μ = 2.46 mm^{-1}, dark blue, hexagonal prism (0.52 × 0.11 × 0.08 mm). Data collection: Stoe IPDS diffractometer, 37137 reflections measured, 12138 independent reflections, R_{int} = 0.0349, 10828 observed reflections ($I_o > 2\sigma(I_o)$), θ_{max} = 25.81°, h = −22 → 22, k = −22 → 21, l = −19 → 19, numerical absorption correction: T_{min} = 0.5006, T_{max} = 0.8340. Refinement: refined on F^2 using all reflections (SHELXL[28]), H-atoms "riding", $wR(F^2)$ = 0.0513, $R(F)$ = 0.0299, S = 0.947, Flack-parameter[24] −0.004(3), 922 parameter, $(\Delta/\sigma)_{max}$ = 0.002, $\Delta\rho_{max}$ = 1.165 e Å^{-3}, $\Delta\rho_{min}$ = −0.422 e Å^{-3}.

Graphics and geometrical parameters were prepared using the PLATON package.[29]

3. Crystal Structures

Within the group−subgroup approach, the symmetry of a known structure is reduced stepwise through substitutions or phase transitions without changing the topology of the packing. The relationships between the structures may be described concisely in a so-called "Bärnighausen family tree".[7] At the top of the tree (Figure 1) resides the structure with the highest symmetry, the so-called "aristotype". From there the symmetry is reduced in minimal steps, so that a parent spacegroup (supergroup) is always followed by maximal subgroups. In the present case, the room-temperature (β) structure of [Ru(bpy)$_3$](PF$_6$)$_2$[30,31] is the aristotype, on the basis of which the topology of the packing will be described in section 3.1. The symmetry reductions are appropriately characterized by the terms "*translationengleich (t)*", "*klassengleich (k)*", and "*isomorph (i)*" and by their index of symmetry reduction. In the first type the subgroup still contains all the translations, but has a crystal class of lower symmetry, while in the latter two cases translational symmetries are lost. Where applicable, new basis vectors for the resulting subgroup are expressed as linear combinations of the parent unit cell (Figure 1), and the three coordinates of a different origin belonging to the subgroup are given with respect to the system of coordinates belonging to the supergroup.

3.1. *β*-[Ru(bpy)$_3$](PF$_6$)$_2$. The room-temperature structure, β-[Ru(bpy)$_3$](PF$_6$)$_2$[30,31] (*P*3*c*1, a = 10.760(1) Å, c = 16.291(3) Å), represents a true racemate. Its unit cell contains one Λ-complex and one Δ-complex, which occupy a special site (Wyckhoff position 2a) with the maximum symmetry (D_3) that may be realized by the chiral [Ru(bpy)$_3$]$^{2+}$ cations (Figure 1). The packing consists of homochiral layers in the *ab*-plane (Figure 2). Λ- and Δ-layers are stacked rigorously alternating along *c* (compare Figure 3). The orientation of the cations is fixed by the site symmetry, the C_3 axis must be collinear with the *c* axis, while the C_2 *a*xes have to be oriented along the hexagonal axes. In the *ab*-plane, the cations do not penetrate each other. Rather, the voids between them are filled with (PF$_6$)$^-$ anions (Figure 2). Alternatively, this structure may be viewed as being built up by heterochiral columns of complex cations stacked with collinear C_3 axes along *c* (Figure 4). Along the column, neighboring cations are interconnected by penetration

(17) (a) Ikeda, N.; Tsushima, M.; Yoshimura, A.; Ohno, T. *Proceedings of the 13th International Symposium on Photochemistry and Photophysics of Coordination Compounds;* Lipari, Italy, 1999; p 60. (b) Gholamkhass, B.; Nozaki, K.; Ohno, T. *J. Phys. Chem. B* **1997**, *101*, 9010.
(18) Shinozaki, K.; Hotta, Y.; Otsuka, T.; Kaizu, Y. *Chem. Lett.* **1999**, 101.
(19) Khan, M. M. T.; Bhardwaj, R. C.; Bhardwaj, C. *Polyhedron* **1990**, *9*, 1243.
(20) Constable, E. C.; Raithby, P. R.; Smit, D. N. *Polyhedron* **1989**, *8*, 367.
(21) Brandt, W. W.; Dwyer, F. P.; Gyarfas, E. C. *Chem. Rev.* **1954**, *54*, 959.
(22) Basolo, F.; Pearson, R. G. *Mechanismen in der anorganischen Chemie*; Georg Thieme Verlag Stuttgart, John Wiley & Sons: Frankfurt, 1973.
(23) Burstall, F. H.; Dwyer, F. P.; Gyarfas, E. C. *J. Chem. Soc.* **1950**, 953.
(24) Flack, H. D. *Acta Crystallogr. A* **1983**, *39*, 876.
(25) Stock, M.; Yersin, H. *Chem. Phys. Lett.* **1976**, *40*, 423.
(26) Yersin, H.; Gliemann, G. *Messtechnik (Braunschweig)* **1972**, *80*, 99.
(27) Huber, P.; Yersin, H. *J. Phys. Chem.* **1993**, *97*, 12705.
(28) Sheldrick, G. M. SHELX-97, University of Göttingen, 1997.
(29) Spek, A. L. *Acta Crystallogr. A* **1990**, *46*, C34.

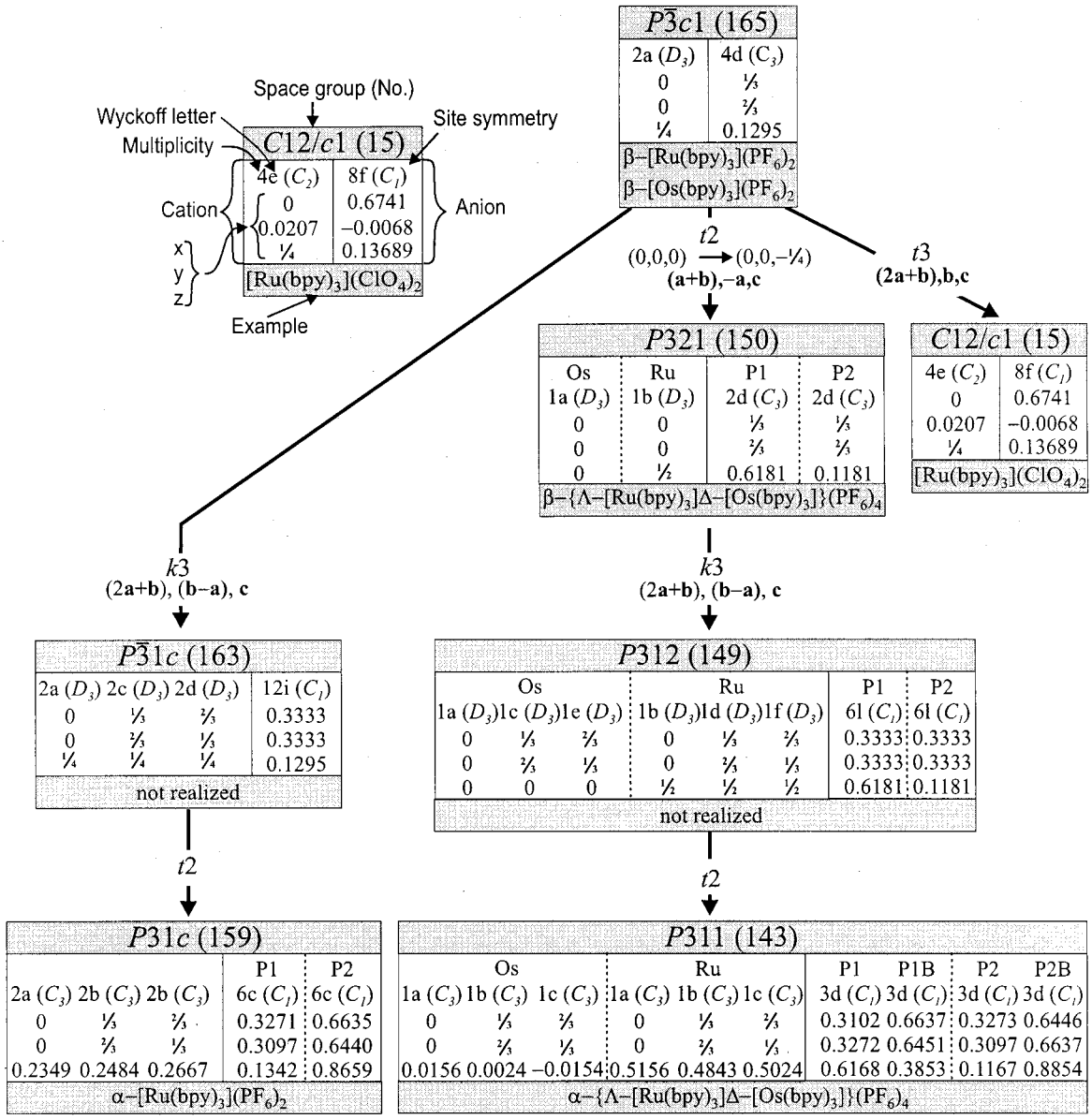

Figure 1. Group−subgroup diagram for the topologically equivalent $[M(bpy)_3]X_2$ structures. "Not realized" structure parameters (coordinates) are idealized and are calculated from the parameters of the super-(parent-)group. Note: Parameters 0, ¼, ½, ... are fixed by symmetry, whereas free parameters are given as decimals (e.g. 0.0000, 0.3333, 0.6667, ...). For reasons of clarity, symmetry equivalent atom positions were preferred on some occasions to those published.

and π-facial hydrogen bonds. In addition to the two cations in the column, each cation is "coordinated" by six anions in a trigonal antiprism. These anions occupy a single special site with the site symmetry C_3 (Wyckhoff position 4d).

The symmetry of this aristotype may be reduced in several ways without changing the topology of the packing of anions and cations.

3.2. *rac*-[Ru(bpy)$_3$](ClO$_4$)$_2$. By exchanging the anion to $(ClO_4)^-$ all 3-fold axes are lost resulting in the *translatio-nengleiche* monoclinic subgroup $C2/c$ of index 3. Thereby, the site symmetry of the $[Ru(bpy)_3]^{2+}$ cations is reduced to C_2. Also, the metric of the unit cell[32,33] is no longer hexagonal, but one finds $b = 10.761(2)$ Å, $a = 17.633(4)$ Å $< b\sqrt{3} = 18.639$ Å, $c = 15.924(4)$ Å, and $\beta = 90.77(2)°$. This indicates that the layers of cations are compressed in the direction of the orthohexagonal *a* axis. Consequently, in the *ab*-plane two sets of Ru−Ru distances result (10.761(2) and 10.329(2) Å). Furthermore, the distance between the $[Ru(bpy)_3]^{2+}$ cations in the column is reduced to 7.962(2) Å as compared to 8.146(2) Å in β-$[Ru(bpy)_3](PF_6)_2$. For the structural parameters of the anions, symmetry restrictions no longer apply, rather they occupy general positions with site symmetry C_1.

3.3. α-[Ru(bpy)$_3$](PF$_6$)$_2$. It is known that by cooling to $T =$ 105 K, the β-$[Ru(bpy)_3](PF_6)_2$ phase undergoes a phase-transition to α-$[Ru(bpy)_3](PF_6)_2$.[34] In the resulting superlattice of the *klassengleiche* maximal subgroup $P\bar{3}1c$ of index 3, three independent $[Ru(bpy)_3]^{2+}$ sites result (Wyckhoff symbol 2a, 2c, 2d). While the anions reside on a general position in this maximal subgroup, all three cation sites still possess D_3 site symmetry and the cations therefore would have exactly the same

(30) Rillema, D. P.; Jones, D. J. *J. Chem. Soc., Chem. Commun.* **1979**, 849.
(31) Rillema, D. P.; Jones, D. S.; Woods, C.; Levy, H. A. *Inorg. Chem.* **1992**, *31*, 2935.
(32) Harrowfield, J. M.; Sobolev, A. N. *Aust. J. Chem.* **1994**, *47*, 763.
(33) Krausz, E.; Riesen, H.; Rae, A. D. *Aust. J. Chem.* **1995**, *48*, 929.
(34) Biner, M.; Bürgi, H.-B.; Ludi, A.; Rohr, C. *J. Am. Chem. Soc.* **1992**, *114*, 5197.

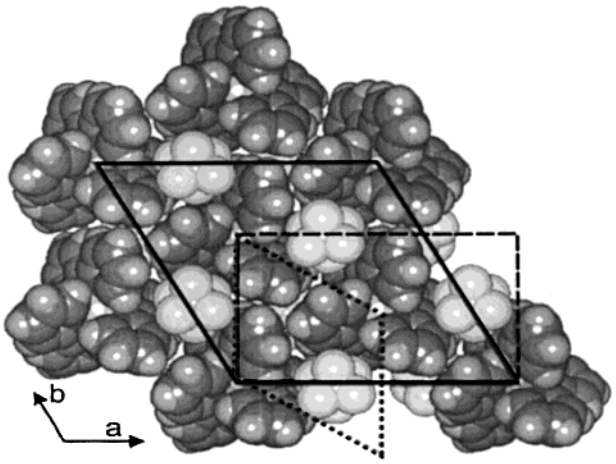

Figure 2. Space-filling packing diagram of a complex cation layer in α-[Ru(bpy)$_3$](PF$_6$)$_2$ or in α-{Λ-[Ru(bpy)$_3$]Δ-[Os(bpy)$_3$]}(PF$_6$)$_4$ (T = 105 K). The dotted line indicates the cell of the room-temperature (β) structure, while the dashed line gives the orientation of the monoclinic unit cell in [Ru(bpy)$_3$](ClO$_4$)$_2$.

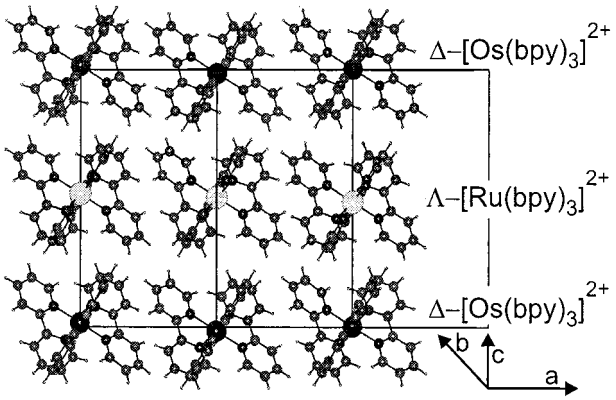

Figure 3. Crystal-packing diagram of the cations in α-{Λ-[Ru(bpy)$_3$]Δ-[Os(bpy)$_3$]}(PF$_6$)$_4$ (T = 105 K). Note the different z coordinates of the three crystallographically distinct [M(bpy)$_3$]$^{2+}$ (M = Ru, Os) cations within a single layer.

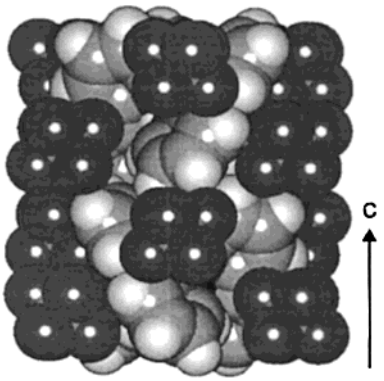

Figure 4. Space-filling packing diagram of heterochiral complex columns stacked along c in the topologically equivalent [M(bpy)$_3$]X$_2$ structures. The diagram displays the interlocking of adjacent cations and their "coordination" by anions.

rotational and translational symmetry as in the room-temperature structure. Probably due to this reason the maximal subgroup is not realized. Instead, the inversion center is also abandoned and α-[Ru(bpy)$_3$](PF$_6$)$_2$ has the *translationengleiche* subgroup $P\bar{3}1c$ of index 2. Thereby, the site-symmetry of the cations (Wyckhoff symbol 2a, 2 × 2b) is reduced to C_3, and the complexes are free to rotate around their C_3 axes (0.7°, 3.6 °, and 4.1 °). Further, they shift slightly along the c axis (0.026, 0.245, and 0.271 Å, compare Figure 3). The c glide plane passes through *0,0,z* interrelating 2a cations within the column, while the 2b sites are projected by symmetry into the neighboring columns. Also, the anion sites split into two crystallographically distinct groups (P1, P2).

3.4. *β*-{Λ-[Ru(bpy)$_3$]Δ-[Os(bpy)$_3$]}(PF$_6$)$_4$. So far, only minor modifications of the structure of highest symmetry have been introduced in the packing and in the relative positions and orientations of [Ru(bpy)$_3$]$^{2+}$. However, by taking advantage of the chirality of these cations a major modification of packing and symmetry reduction may be "forced" upon the system.

It has been shown that [Os(bpy)$_3$](PF$_6$)$_2$ is isomorphous[20,35] with [Ru(bpy)$_3$](PF$_6$)$_2$. When doping β-[Ru(bpy)$_3$](PF$_6$)$_2$ with racemic [Os(bpy)$_3$](PF$_6$)$_2$ both Λ- and Δ-[Ru(bpy)$_3$]$^{2+}$ are replaced by [Os(bpy)$_3$]$^{2+}$ in the resulting solid solution. However, when doping with Δ-[Os(bpy)$_3$]$^{2+}$ it can only be incorporated in the Δ-sites of the packing and therefore only in every second layer. Furthermore, pseudoracemic 1:1 mixtures of Λ-[Ru(bpy)$_3$](PF$_6$)$_2$ and Δ-[Os(bpy)$_3$](PF$_6$)$_2$ (or vice versa) must crystallize in the *translationengleiche* subgroup $P321$ if the topology of the packing is preserved. Λ- and Δ-layers now consist of different cations though of very similar sizes and shapes. As an important consequence, close Ru−Ru or Os−Os contacts now exist only in the *ab* plane (≈10.6 Å, Figure 2), but along the columns (Figures 3 and 4) Λ-[Ru(bpy)$_3$]$^{2+}$ and Δ-[Os(bpy)$_3$]$^{2+}$ alternate rigorously. Utilization of chirality allows for a controlled symmetry reduction resulting in a crystal that is built up from alternating [Ru(bpy)$_3$]$^{2+}$ and [Os(bpy)$_3$]$^{2+}$ layers (Figure 3). The site symmetries of both cations in this room-temperature (β) structure are D_3 as in pure [Ru(bpy)$_3$](PF$_6$)$_2$, but the Λ- and Δ-sites are no longer connected via glide planes. The anion sites split into two crystallographically distinct groups, but still possess C_3 site symmetry. The P1 and P2 sites are surrounding the Ru and Os cations, respectively.

3.5. α-{Λ-[Ru(bpy)$_3$]Δ-[Os(bpy)$_3$]}(PF$_6$)$_4$. β-{Λ-[Ru(bpy)$_3$]Δ-[Os(bpy)$_3$]}(PF$_6$)$_4$ undergoes a phase transition upon cooling (T = 105 K) in analogy to β-[Ru(bpy)$_3$](PF$_6$)$_2$. For the same reason as given above, the *klassengleiche* maximal subgroup of index 3 is not realized. Loss of all 2-fold axes gives rotational and translation degrees of freedom to the cations. They rotate around their C_3 axis (Ru: 0.9°, 3.5°, 4.1°; Os: 0.8°, 3.5°, 4.3°) and are displaced along the c axis (Ru: 0.039, 0.253, 0.254 Å; Os: 0.039, 0.250, 0.253 Å). Thus, three distinct crystallographic sites each exist for Λ-[Ru(bpy)$_3$]$^{2+}$ and Δ-[Os(bpy)$_3$]$^{2+}$ in the Λ- and the Δ-layer, respectively. The anions occupy four different general positions (P1, P1B, P2, P2B). Since the transition from $P312$ to $P311$ is of the type *translationengleich*, α-{Λ-[Ru(bpy)$_3$]Δ-[Os(bpy)$_3$]}(PF$_6$)$_4$ has to be refined as a twin.[7,36]

4. Radiationless Energy Transfer

4.1. ^{3}MLCT Emissions of [Ru(bpy)$_3$]$^{2+}$ and [Os(bpy)$_3$]$^{2+}$. Properties of the low-lying states and in particular the emission behavior of [Ru(bpy)$_3$]$^{2+}$ and [Os(bpy)$_3$]$^{2+}$ have already been studied in detail elsewhere (see reviews 9 and 37 and references therein). Therefore, here only a short introduction is presented. The lower excited states can be related in a first approximation to orbital jumps from the Ru(4dπ) and Os(5dπ) HOMO, respectively, to the bpy(π*) LUMO. Thus, the resulting excited

(35) Richter, M. M.; Scott, B.; Brewer, K. J.; Willett, R. D. *Acta Crystallogr. C* **1991**, *47*, 2443.
(36) Herbst-Irmer, R.; Sheldrick, G. M. *Acta Crystallogr. B* **1998**, *54*, 443.

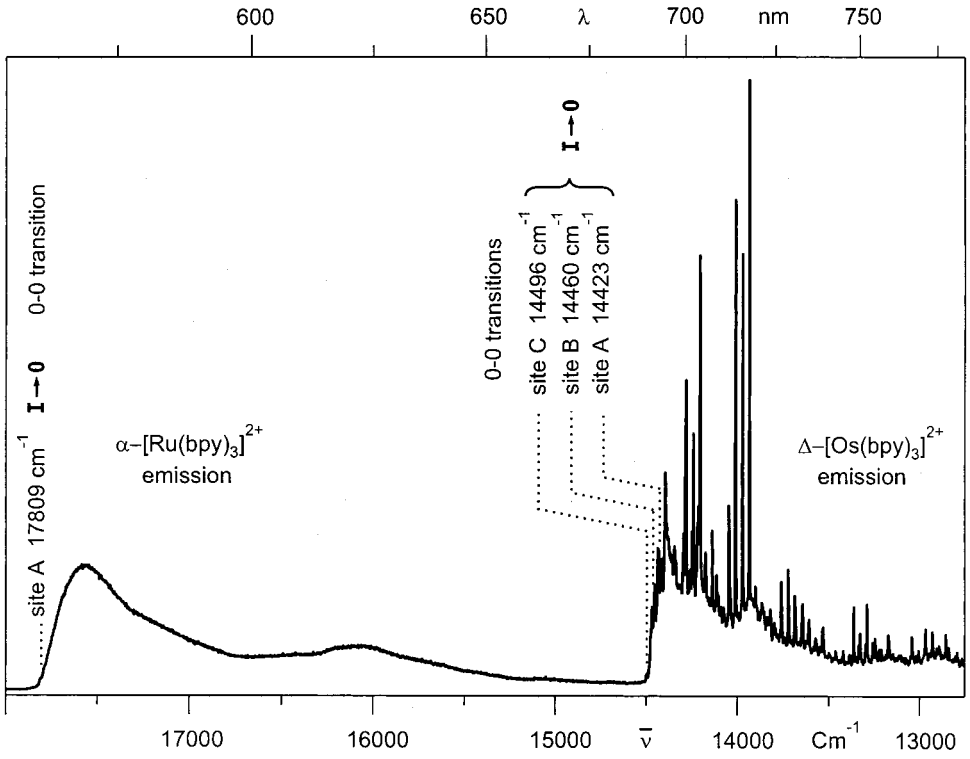

Figure 5. Emission of α-$[Ru(bpy)_3](PF_6)_2$ doped with 1% Δ-$[Os(bpy)_3]^{2+}$ (mol/mol) ($T = 1.3$ K, $\lambda_{exc} = 457.9$ nm). The lowest electronic origins of the different emitters are indicated. The emission of Δ-$[Os(bpy)_3]^{2+}$ is reproduced also in an enlarged scale in Figure 6a.

states are classified as metal-to-ligand charge-transfer (MLCT) states, namely ^{1}MLCT and ^{3}MLCT states, while the ground state is a singlet. The emissions of both compounds result from the lowest ^{3}MLCT states. These are split by spin−orbit coupling into sublevels **I**, **II**, and **III**, of which at low temperature mainly the lowest substates **I** emit.[9] The emission properties slightly depend on the solid-state matrix. For example, for $[Ru(bpy)_3]^{2+}$ the lowest electronic origin (0−0 transition) shifts from 17809 to 17605 cm^{-1}, when going from α-$[Ru(bpy)_3](PF_6)_2$ to the distorted (see section 3.2) *rac*-$[Ru(bpy)_3](ClO_4)_2$,[9,37] while for $[Os(bpy)_3]^{2+}$ doped into these different matrixes the electronic origins are shifted from 14423 to 14169 cm^{-1}.[9,38]

For a *low* concentration of Δ-$[Os(bpy)_3]^{2+}$ in α-$[Ru(bpy)_3](PF_6)_2$ one observes emissions of both compounds (Figure 5). The spectra lie in different energy ranges and therefore can be well distinguished from each other. The emission of $[Ru(bpy)_3](PF_6)_2$ (doped with Δ-$[Os(bpy)_3]^{2+}$ guest molecules) is broad and not well resolved due to effects of inhomogeneous broadenings, overlapping vibrational satellites, and relatively strong phonon couplings. Although three crystallographic sites of $[Ru(bpy)_3]^{2+}$ are present (see section 3.3), the spectrum consists nearly exclusively of the emission of one single site, A(Ru). (See the next section and refs 9 and 39.) On the other hand, the vibrational satellites of Δ-$[Os(bpy)_3]^{2+}$ are well resolved, due to a weaker coupling to the lattice. However, the spectrum is built up from overlapping emissions of three different sites A(Os), B(Os), and C(Os). The emission spectrum is very similar to the one found for doping with *rac*-$[Os(bpy)_3]^{2+}$ (refs 9 and 40). An assignment of these spectroscopically identified sites to crystallographic positions, as described in section 3.3, is not yet possible.

4.2. Energy Transfer in α-$[Ru(bpy)_3](PF_6)_2$ Doped with Δ-$[Os(bpy)_3]^{2+}$. At *low* concentrations of Δ-$[Os(bpy)_3]^{2+}$ guests, the excitation is predominantly absorbed by the $[Ru(bpy)_3]^{2+}$ host material, even when an excitation wavelength is chosen at which both compounds absorb. Subsequently, excitation energy is transferred radiationlessly from the host (donor) to the Δ-$[Os(bpy)_3]^{2+}$ guest complexes (acceptors). The occurrence of radiationless processes is concluded from the following results:

(1) The emission intensity of the host material is strongly reduced when Δ-$[Os(bpy)_3]^{2+}$ dopants are present. For example, a doping of 0.1% and 1%, respectively, quenches the emission intensity (at $T = 1.3$ K) of the host material by ≈30% and ≈60%, respectively, compared with neat α-$[Ru(bpy)_3](PF_6)_2$.[41]

(2) The emission decay time of the host material is significantly reduced by doping of Δ-$[Os(bpy)_3]^{2+}$, and the emission decay becomes nonmonoexponential. The long decay component decreases from 250 μs (decay time of state **I** of neat α-$[Ru(bpy)_3](PF_6)_2$ at $T = 1.3$ K)[9] to 225 μs (0.1% $[Os(bpy)_3]^{2+}$), to 110 μs (1%), and to 75 μs (2%).[41]

(3) When the excitation wavelength of $\lambda_{exc} = 457.9$ nm is chosen, at which mainly α-$[Ru(bpy)_3](PF_6)_2$ is excited due to the high concentration of the host material, the decay time of the Δ-$[Os(bpy)_3]^{2+}$ emission is relatively long and very similar to that of the host material, since the donor is representing a long-lived reservoir. By use of a selective excitation of Δ-$[Os(bpy)_3]^{2+}$ with $\lambda_{exc} = 675$ nm one obtains the much shorter decay time of the dopant itself of $\tau = (22 \pm 1)$ μs (decay time of state **I** at $T = 1.3$ K, compare also ref 27).

The properties described can be rationalized by a model, which ignores transfer processes between the acceptor complexes due to the small doping concentration of Δ-$[Os(bpy)_3]^{2+}$,

(37) Yersin, H.; Braun, D.; Hensler, G.; Gallhuber, E. In *Vibronic Processes in Inorganic Chemistry*; Flint, C. D., Ed.; Kluwer Academic Press: Dordrecht, 1989; p 195.
(38) Yersin, H.; Gallhuber, E.; Hensler, G. *Chem. Phys. Lett.* **1987**, *140*, 157.
(39) Braun, D.; Yersin, H. *Inorg. Chem.* **1995**, *34*, 1967.
(40) Braun, D.; Gallhuber, E.; Hensler, G.; Yersin, H. *Mol. Phys.* **1989**, *67*, 417.
(41) Otte, M. Diplomarbeit, Universität Regensburg, 1992.

but which takes into account two other processes of energy transfer: (1) donor−donor processes of excitation transfer and (2) processes of donor−acceptor radiationless energy transfer.

Obviously, the donor−donor transfer is not very efficient, since one needs relatively high acceptor concentrations to quench the donor emission when compared to other single-crystal compounds, in which several orders of magnitude smaller amounts of dopants already drastically quench the donor emission.[42,43] Moreover, the information available from ref 39 shows clearly that the energy transfer between the $[Ru(bpy)_3]^{2+}$ sites is composed of different processes, since three different sites A(Ru), B(Ru), and C(Ru) are present. (Compare Figure 6a.) Energetically they are separated by (19 ± 1) cm^{-1} from each other.[39] The rate of energy transfer from site B(Ru) to the lowest site A(Ru) has been determined for neat α-[Ru(bpy)$_3$](PF$_6$)$_2$ to be 1.7×10^7 s^{-1} (60 ns),[9,39] while the rates for the processes from site C(Ru) to the sites A(Ru) and B(Ru), respectively, are so fast that the emission of site C(Ru) is totally quenched. Only a lower limit for the quenching rate of site C(Ru) of ≈10^8 s^{-1} may be estimated.

From these considerations it follows that the excitation is at first transferred to site A(Ru) of lowest energy of α-[Ru(bpy)$_3$](PF$_6$)$_2$. However, then the donor−donor transfer between inhomogeneously distributed site A(Ru) positions will not be very efficient, since such processes are not really in resonance. They are slowed due to an energy mismatch (e.g. compare ref 44) of the order of the inhomogeneous line width of the corresponding transition **I** ↔ **0** (≈4 cm^{-1} at $T = 1.3$ K).[9]

For completeness it is mentioned that the processes of energy transfer are also influenced by the second lowest triplet substate **II** of the host compound. This substate lies 6.9 cm^{-1} above state **I**. Both states are thermally *not* equilibrated at $T = 1.3$ K due to a relatively slow spin−lattice relaxation time of 250 ns.[9,45] Therefore, both donor states are (differently) involved in the transfer processes.[11] However, a detailed analysis of these donor (site A)−donor (site A) hopping processes is far beyond the present report.

Finally, when after a relatively slow hopping process the excitation comes near an Δ-$[Os(bpy)_3]^{2+}$ acceptor, the $[Ru(bpy)_3]^{2+} \rightarrow [Os(bpy)_3]^{2+}$ energy transfer is fast, as is reflected in the fast decaying component of the $[Ru(bpy)_3]^{2+}$ donor emission (not reproduced, compare also the results presented in section 4.3). The mechanism of this transfer process (Förster multipole or Dexter exchange)[46] has not yet been determined, but it is evident that the resonance condition is well fulfilled, since one has a very good spectral overlap between the $[Ru(bpy)_3]^{2+}$ donor emission (for all three sites) and the Δ-$[Os(bpy)_3]^{2+}$ acceptor absorption.[9,10] The occurrence of a fast transfer process from a $[Ru(bpy)_3]^{2+}$ donor to a nearest $[Os(bpy)_3]^{2+}$ neighbor is also reported in ref 17a for a slightly different system, for which a transfer rate of 10^{10} s^{-1} is estimated.

4.3. Intralayer Transfer between Δ-[Os(bpy)$_3$]$^{2+}$ Sites. At *high* concentrations of Δ-$[Os(bpy)_3]^{2+}$ as is realized in the newly engineered {Λ-[Ru(bpy)$_3$] Δ-[Os(bpy)$_3$]}(PF$_6$)$_4$ compound one has to take into account that an excitation at shorter wavelengths (e.g. at $\lambda_{exc} = 457.9$ nm) will always excite both chromophores. Thus, the lowest triplet sublevels of Δ-$[Os(bpy)_3]^{2+}$ will be populated by processes of intersystem crossing from higher lying singlets of Δ-$[Os(bpy)_3]^{2+}$ itself and by processes of energy transfer from Λ-$[Ru(bpy)_3]^{2+}$ as discussed in the previous section. These latter processes lead to a complete quenching of the emission of Λ-$[Ru(bpy)_3]^{2+}$, which again indicates fast processes of energy transfer from the Λ-$[Ru(bpy)_3]^{2+}$ chromophores to Δ-$[Os(bpy)_3]^{2+}$.

Moreover, the Δ-$[Os(bpy)_3]^{2+}$ spectrum changes characteristically, when compared to the situation at low concentration (compare parts a and b in Figure 6). Interestingly, for a high concentration of $[Os(bpy)_3]^{2+}$, the spectrum becomes much simpler. An emission spectrum results that is similar to the one measured at low concentration, but for which only site A of $[Os(bpy)_3]^{2+}$ is selectively excited (see refs 9 and 40). Obviously, efficient processes of energy transfer occur between the different Δ-$[Os(bpy)_3]^{2+}$ sites. As a consequence, the emissions of the sites B(Os) and C(Os) are totally quenched by transfer processes to the low-lying spectroscopic site A(Os).

The emission decay time of this site A(Os) is 22 μs (at $T =$ 1.3 K). The same value has also been found for the doped Δ-$[Os(bpy)_3]^{2+}$ complex. Moreover, the decay time is independent of the excitation wavelength. This means that the same value is obtained, when site A(Os) is excited directly, when the sites B(Os) and C(Os) are excited, or also when higher lying states of the Λ-$[Ru(bpy)_3]^{2+}$ chromophores are excited (Figure 7). This behavior allows us to conclude that the excitation energy is transferred from all other units to the spectroscopic site A(Os) of Δ-$[Os(bpy)_3]^{2+}$. Very probably, the Δ-$[Os(bpy)_3]^{2+} \rightarrow$ Δ-$[Os(bpy)_3]^{2+}$ energy transfer proceeds within a homochiral layer, where the different Δ-$[Os(bpy)_3]^{2+}$ sites are direct neighbors, while Δ-$[Os(bpy)_3]^{2+}$ sites of different layers have larger separations (16.2 Å) due to Λ-$[Ru(bpy)_3]^{2+}$ layers lying between them (section 3.5).

The intralayer energy transfers between nearest neighbors of Δ-$[Os(bpy)_3]^{2+}$ from the sites C(Os) and B(Os) to site A(Os) are possible as resonance processes. This becomes clear when considering that the emissions of the energetically higher lying sites C(Os) and B(Os) donors exhibit nonvanishing spectral overlaps (compare ref 46) with the absorption of the acceptor site A(Os). Figure 6a shows the positions of the corresponding electronic origins and it is seen that those of the higher lying sites are shifted by 36 and 73 cm^{-1}, respectively, relative to the origin of site A(Os). A transfer mechanism according to a multipole process, in particular, to a dipole−dipole transfer, seems to be very inefficient due to the extremely low absorption probability (oscillator strength) of the **0** → **I** transition at 14412 cm^{-1} of the acceptor site A(Os). (This electronic 0−0 transition is strongly forbidden, see also refs 9 and 40.) Moreover, due to the relatively small separations between the outer parts of the ligands of different Δ-$[Os(bpy)_3]^{2+}$ complexes within a layer (less than 1 Å), the tails of the wave functions of the ^{3}MLCT states, being involved in the transfer processes, probably still experience some overlap. In this situation the Dexter exchange mechanism of energy transfer can be very efficient.[46] This fits well to the observation that the emissions of the higher lying sites C(Os) and B(Os) are totally quenched.

The electronic origin of site A(Os) of lowest energy of the title compound is found at (14412 ± 2) cm^{-1} (Figure 6b). Interestingly, this transition is shifted by ≈11 cm^{-1} to lower energy relative to the electronic origin at (14423 ± 1) cm^{-1} (refs 9, 40, and 47) of site A(Os) of Δ-$[Os(bpy)_3]^{2+}$ doped with a small concentration into the α-$[Ru(bpy)_3](PF_6)_2$ matrix.

(42) Holzapfel, W.; Yersin, H.; Gliemann, G. *J. Chem. Phys.* **1981**, *74*, 2124.
(43) Köhler, M.; Schmid, D.; Wolf, H. C. *J. Luminesc.* **1976**, *14*, 41.
(44) Henderson, B.; Imbusch, G. F. *Optical Spectroscopy of Inorganic Solids*; Clarendon Press: Oxford, 1989; p 466.
(45) Yersin, H.; Strasser, J. *J. Luminesc.* **1997**, *72−74*, 462.
(46) Dexter, D. L. *J. Chem. Phys.* **1953**, *21*, 836.
(47) Braun, D.; Hensler, G.; Gallhuber, E.; Yersin, H. *J. Phys. Chem.* **1991**, *95*, 1067.

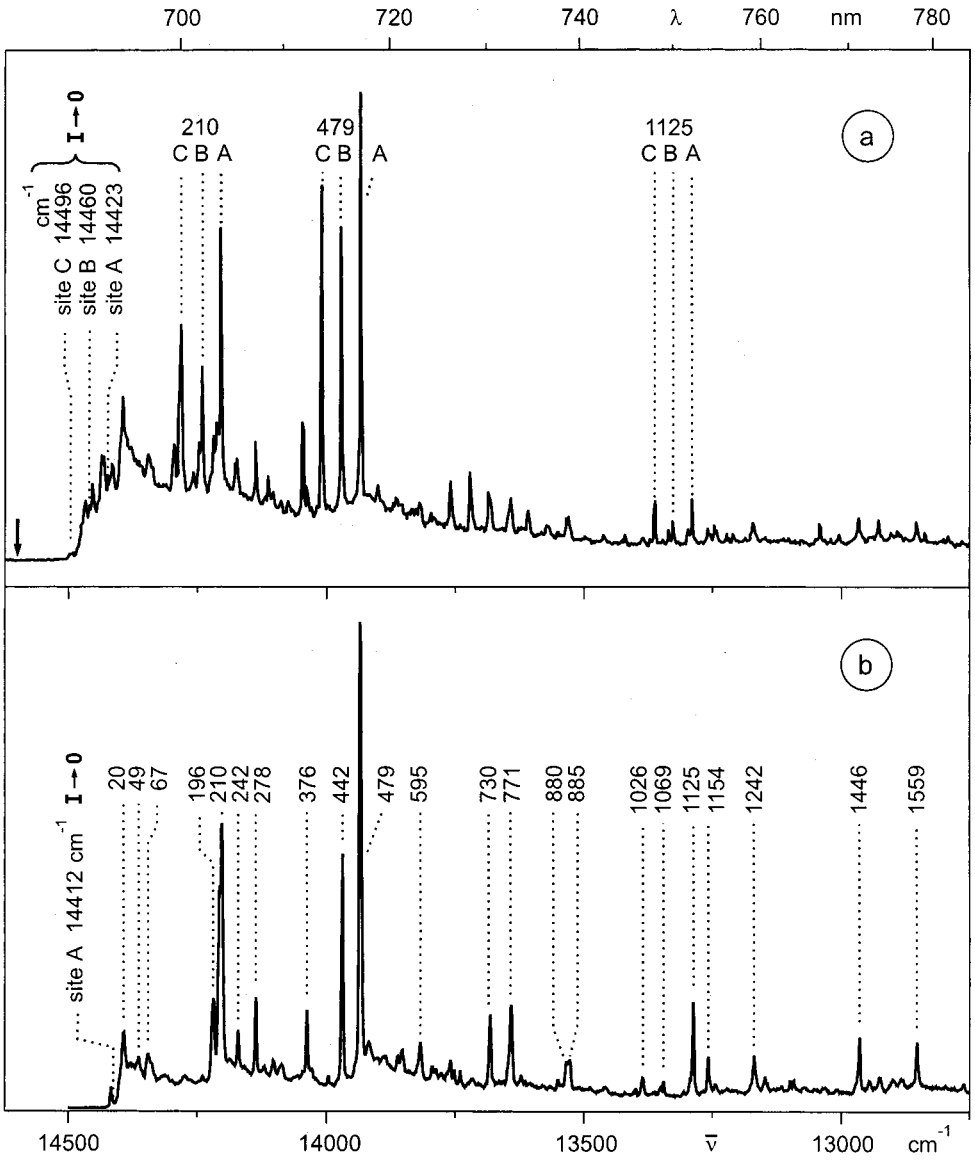

Figure 6. (a) Emission of 1% Δ-$[Os(bpy)_3]^2$ (mol/mol) doped into α-$[Ru(bpy)_3](PF_6)_2$ (T = 1.3 K). The same spectrum is also reproduced in Figure 5, but here an enlarged scale is used for comparison. Near 14600 cm^{-1} one observes the low-energy tail of the $[Ru(bpy)_3]^{2+}$ emission (see arrow). (b) Emission spectrum of neat {Λ-$[Ru(bpy)_3]$Δ-$[Os(bpy)_3]$}$(PF_6)_4$ at T = 1.3 K. The emission results only from the site of lowest energy of Δ-$[Os(bpy)_3]^{2+}$ (site A(Os)), although the compound is nonselectively excited at λ_{exc} = 457.9 nm. Due to different processes of radiationless energy transfer the whole excitation energy is accumulated on this site.

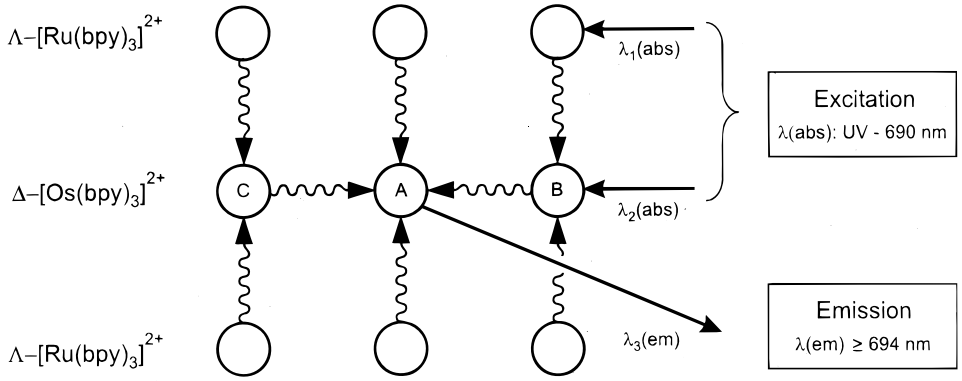

Figure 7. Schematic diagram of absorption, radiationless energy transfer, and emission processes in α-{Λ-$[Ru(bpy)_3]$Δ-$[Os(bpy)_3]$}$(PF_6)_4$. The diagram shows that by processes of radiationless energy transfer the excitation energy is harvested by the site of lowest energy of Δ-$[Os(bpy)_3]^{2+}$ (site A).

This energy shift seems to reflect the slightly different structure parameters of α-$[Ru(bpy)_3](PF_6)_2$ as compared to the title compound.

The vibrational satellite structure, which is well resolved in the emission spectrum of site A(Os) (Figure 6b), is similar to the structure of *rac*-$[Os(bpy)_3]^{2+}$ doped into α-$[Ru(bpy)_3](PF_6)_2$

(compare Figure 6b to refs 9, 40, and 47). Therefore, an assignment of the vibrational satellites is straightforward. The low-energy satellites up to ≈100 cm^{-1} relative to the electronic origin at 14412 cm^{-1} correspond to or are influenced by lattice modes. These are slightly shifted to lower energy for the title compound, presumably due to its higher mass compared to α-[Ru(bpy)$_3$](PF$_6$)$_2$. Satellites in the energy range $\approx 100 \leq \bar{\nu} \leq \approx 600$ cm^{-1} (relative to the electronic origin) correspond to metal−ligand vibrations, and those above ≈600 cm^{-1} are assigned to internal ligand vibrations. In particular, due to the observation that usually the frequencies of internal ligand vibrations exhibit only very small shifts (if at all), when chromophores are built into different matrices (see refs 9, 40, and 48), these values may be applied to determine the energy position of an electronic origin. This procedure is of particular use when the transition at the origin is totally forbidden, as is found here (Figure 6b). Due to this forbiddenness it may also be concluded that the vibrational satellites observed are all vibronically (Herzberg−Teller) induced. (For details compare refs 9, 40, 47, and 49.)

5. Conclusion

The presented example shows that for highly symmetric molecular solids the group−subgroup approach may be an efficient design strategy to arrive at new crystal structures with specific physical properties. Moreover, this approach does not rely on classical hydrogen bonds that represent the strongest, most directional and reliable noncovalent forces. Rather, as in the presented example, dispersion and weak $\pi-\pi$ interactions are sufficient since the topology is only altered but not completely changed. Since [Os(bpy)$_3$]$^{2+}$ and [Ru(bpy)$_3$]$^{2+}$ are so similar in molecular shape they cannot be distinguished in the self-assembly of the crystal. By taking advantage of their configurational stability, it becomes feasible to engineer a structure that consists of rigorously alternating homochiral layers of Λ-[Ru(bpy)$_3$]$^{2+}$ and Δ-[Os(bpy)$_3$]$^{2+}$ (or vice versa).

This crystalline system exhibits a number of interesting new properties, in particular, with respect to the interplay of interlayer and intralayer radiationless energy transfer. Figure 7 summarizes these aspects schematically. The excitation, which is absorbed in the energy range from the UV to the red side of the visible by both [Ru(bpy)$_3$]$^{2+}$ and [Os(bpy)$_3$]$^{2+}$, is accumulated at the site of lowest energy of Δ-[Os(bpy)$_3$]$^{2+}$. Due to the specific structure, this site is well isolated with respect to further processes of energy transfer and therefore one observes an intense emission only of this site, irrespective of the applied excitation wavelength. Moreover, since this emission is site-selected and highly resolved the spectrum reflects detailed electronic and vibronic properties of Δ-[Os(bpy)$_3$]$^{2+}$.

Acknowledgment. J.B. would like to thank Prof. Dr. K.-J. Range for making equipment available and miscellaneous support. We further thank Dr. M. Zabel for valuable discussions and for measuring one of the data sets. Financial support by the Fonds der Chemischen Industrie and the DFG is acknowledged. Also, we thank the Degussa AG for a donation of RuCl$_3$·3H$_2$O and OsCl$_3$.

Supporting Information Available: Crystallographic data including details of the crystal structure refinement, atomic parameters, bond lengths and angles, anisotropic displacement parameters, and hydrogen parameters (PDF). This material is available free of charge via the Internet at http://pubs.acs.org.

JA993104M

(48) Yersin, H.; Trümbach, D.; Wiedenhofer, H. *Inorg. Chem.* **1999**, *38*, 1411.

(49) Albrecht, A. C. *J. Chem. Phys.* **1963**, *38*, 354.